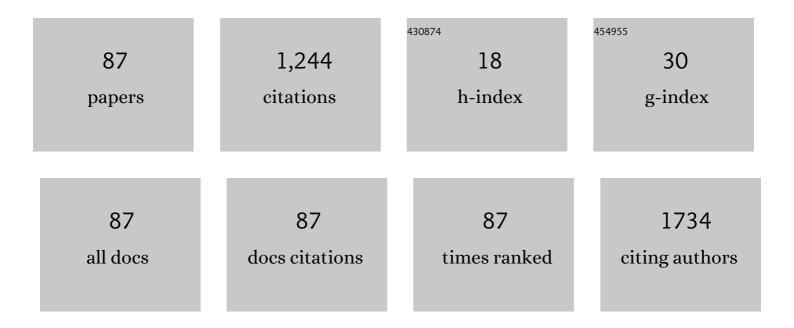
Thanh-Huy Pham

List of Publications by Year in descending order

Source: https://exaly.com/author-pdf/1724973/publications.pdf Version: 2024-02-01



#	Article	IF	CITATIONS
1	Strong Rashbaâ€Dresselhaus Effect in Nonchiral 2D Ruddlesdenâ€Popper Perovskites. Advanced Optical Materials, 2022, 10, 2101232.	7.3	14
2	Synthesis, structural and optical properties of ZnS/ZnO heterostructure-alloy hexagonal micropyramids. Optical Materials, 2022, 125, 112077.	3.6	4
3	MnP Films with Desired Magnetic, Magnetocaloric, and Thermoelectric Properties for a Perspective Magnetoâ€Thermoâ€Electric Cooling Device. Physica Status Solidi (A) Applications and Materials Science, 2022, 219, 2100367.	1.8	1
4	Orangeâ€Redâ€emitting Ca ₉ Gd(PO ₄) ₇ :Eu ³⁺ Phosphors: Juddâ€Ofelt Analysis and Investigation on the Thermal Stability, Quantum Efficiency for WLED. ChemistrySelect, 2021, 6, 937-944.	1.5	6
5	Pd ₈₀ Co ₂₀ Nanohole Arrays Coated with Poly(methyl methacrylate) for High-Speed Hydrogen Sensing with a Part-per-Billion Detection Limit. ACS Applied Nano Materials, 2021, 4, 3664-3674.	5.0	5
6	Strain-modulated helimagnetism and emergent magnetic phase diagrams in highly crystalline MnP nanorod films. Physical Review B, 2021, 103, .	3.2	6
7	Emission-tunable Mn-doped ZnS/ZnO heterostructure nanobelts for UV-pump WLEDs. Optical Materials, 2021, 121, 111587.	3.6	14
8	Enhanced thermoelectric properties of Hf-free half-Heusler compounds prepared via highly fast process. Journal of Alloys and Compounds, 2021, 886, 161293.	5.5	6
9	Single-composition Al ³⁺ -singly doped ZnO phosphors for UV-pumped warm white light-emitting diode applications. Dalton Transactions, 2021, 50, 9037-9050.	3.3	12
10	A high quantum efficiency plant growth LED by using a deep-red-emitting α-Al ₂ O ₃ :Cr ³⁺ phosphor. Dalton Transactions, 2021, 50, 12570-12582.	3.3	28
11	Mn2+- doped Zn2SnO4 green phosphor for WLED applications. Journal of Luminescence, 2020, 227, 117522.	3.1	18
12	Synthesis and Photoluminescence Properties of Deep-Red-Emitting CaYAlO4:Cr3+ Phosphors. Journal of Electronic Materials, 2020, 49, 7464-7471.	2.2	7
13	Structural relaxation time and dynamic shear modulus of glassy graphene. Journal of Non-Crystalline Solids, 2020, 538, 120024.	3.1	4
14	A magnetic sensor using a 2D van der Waals ferromagnetic material. Scientific Reports, 2020, 10, 4789.	3.3	23
15	Origin of Rashba Spin-Orbit Coupling in 2D and 3D Lead Iodide Perovskites. Scientific Reports, 2020, 10, 4964.	3.3	23
16	Photoluminescent properties of red-emitting phosphor BaMgAl10O17:Cr3+ for plant growth LEDs. Optical Materials, 2020, 108, 110207.	3.6	35
17	Facile synthesis of single phase α-Zn2SiO4:Mn2+ phosphor via high-energy planetary ball milling and post-annealing method. Journal of Luminescence, 2019, 215, 116612.	3.1	21
18	X-site aliovalent substitution decoupled charge and phonon transports in XYZ half-Heusler thermoelectrics. Acta Materialia, 2019, 166, 650-657.	7.9	10

#	Article	IF	CITATIONS
19	Deep Red Emitting MgAl2O4:Cr3+ Phosphor for Solid State Lighting. Journal of Electronic Materials, 2019, 48, 5891-5899.	2.2	19
20	Magnetically tunable organic semiconductors with superparamagnetic nanoparticles. Materials Horizons, 2019, 6, 1913-1922.	12.2	5
21	High thermoelectric power factor in SnSe ₂ thin film grown on Al ₂ O ₃ substrate. Materials Research Express, 2019, 6, 066420.	1.6	4
22	Surface oxygen vacancies of ZnO: A facile fabrication method and their contribution to the photoluminescence. Journal of Alloys and Compounds, 2019, 791, 722-729.	5.5	63
23	Synthesis and thermoelectric properties of Ti-substituted (Hf0.5Zr0.5)1-xTixNiSn0.998Sb0.002 Half-Heusler compounds. Journal of Alloys and Compounds, 2019, 773, 1141-1145.	5.5	13
24	Excitation energy dependence of the life time of orange emission from Mn-doped ZnS nanocrystals. Journal of Luminescence, 2018, 199, 39-44.	3.1	13
25	Local Structure and Chemistry of Câ€Doped ZnO@C Core–Shell Nanostructures with Roomâ€Temperature Ferromagnetism. Advanced Functional Materials, 2018, 28, 1704567.	14.9	17
26	Controlling Blue and Red Light Emissions from Europium (Eu2+)/Manganese (Mn2+)-Codoped Beta-Tricalcium Phosphate [l²-Ca3(PO4)2 (TCP)] Phosphors. Journal of Electronic Materials, 2018, 47, 2964-2969.	2.2	6
27	In situ observation of phase transformation in iron carbide nanocrystals. Micron, 2018, 104, 61-65.	2.2	4
28	Correlation length in a generalized two-dimensional XY model. Physical Review B, 2018, 98, .	3.2	13
29	Effect of doping concentration and sintering temperature on structure and photoluminescence properties of blue/red emitting bi-phase Eu ³⁺ /Eu ²⁺ -doped Sr ₅ (PO ₄) ₃ Cl/Sr ₃ (PO ₄) ₂ phosphors. Materials Research Express, 2018, 5, 076516.	1.6	5
30	Hydrothermal synthesis, structure, and photocatalytic properties of SnO ₂ /rGO nanocomposites with different GO concentrations. Materials Research Express, 2018, 5, 095506.	1.6	14
31	A versatile approach to synthesise optically active hierarchical ZnS/ZnO heterostructures. International Journal of Nanotechnology, 2018, 15, 222.	0.2	0
32	Achieving High Luminescent Performance K2SiF6:Mn4+ Phosphor by Co-precipitation Process with Controlling the Reaction Temperature. Journal of Electronic Materials, 2018, 47, 4634-4641.	2.2	4
33	Effect of potting materials on LED bulb's driver temperature. Microelectronics Reliability, 2018, 86, 77-81.	1.7	4
34	Luminescence of Nanoporous Si and ALD-Deposited ZnO on Nanoporous Si Substrate. Journal of Electronic Materials, 2017, 46, 4784-4790.	2.2	1
35	Sol–gel synthesis and photoluminescence of SiO ₂ –Si:Er ³⁺ nanocomposite films. Materials Research Express, 2017, 4, 036205.	1.6	2
36	Influence of Annealing Temperature and Gd and Eu Concentrations on Structure and Luminescence Properties of (Y,Gd)BO3:Eu3+ Phosphors Prepared by Sol–Gel Method. Journal of Electronic Materials, 2017, 46, 3427-3432.	2.2	3

#	Article	IF	CITATIONS
37	Lasing from ZnO Nanocrystals in ZnO-ZnS Microbelts. Journal of Electronic Materials, 2017, 46, 3295-3300.	2.2	6
38	Enhancing the luminescence of Eu ³ ⁺ /Eu ² ⁺ ionâ€doped hydroxyapatite by fluoridation and thermal annealing. Luminescence, 2017, 32, 817-823.	2.9	14
39	Enhanced ferromagnetism in graphite-like carbon layer-coated ZnO crystals. Journal of Alloys and Compounds, 2017, 695, 233-237.	5.5	6
40	Understanding ferromagnetism in C-doped CdS: Monte Carlo simulation. Journal of Alloys and Compounds, 2017, 695, 1624-1630.	5.5	11
41	Effect of substrate temperature on structural and optical properties of ZnO nanostructures grown by thermal evaporation method. Physica E: Low-Dimensional Systems and Nanostructures, 2017, 85, 174-179.	2.7	9
42	Synthesis and optical properties of red/blue-emitting Sr2MgSi2O7:Eu3+/Eu2+ phosphors for white LED. Journal of Science: Advanced Materials and Devices, 2016, 1, 204-208.	3.1	13
43	Structural evolution and optical properties of oxidized ZnS microrods. Journal of Alloys and Compounds, 2016, 676, 150-155.	5.5	13
44	Synthesis and Optical Properties of Eu2+ and Eu3+ Doped SrBP Phosphors Prepared by Using a Co-precipitation Method for White Light-Emitting Devices. Journal of Electronic Materials, 2016, 45, 3356-3360.	2.2	8
45	Photoluminescence and Cathodoluminescence Characterization of Ge/GeO2 Nanostructure Synthesized by Thermal Evaporation of Ge Powder. Journal of Applied Spectroscopy, 2016, 83, 665-668.	0.7	Ο
46	Luminescence of one dimensional ZnO, GeO2–Zn2GeO4 nanostructure through thermal evaporation of Zn and Ge powder mixture. Materials Science and Engineering B: Solid-State Materials for Advanced Technology, 2016, 209, 17-22.	3.5	11
47	Effects of carbon on optical properties of ZnO powder. Journal of Luminescence, 2016, 174, 6-10.	3.1	35
48	Magnetic properties of sol-gel synthesized C-doped ZnO nanoparticles. Journal of Alloys and Compounds, 2016, 668, 87-90.	5.5	37
49	Probing the origin of green emission in 1D ZnS nanostructures. Journal of Luminescence, 2016, 169, 165-172.	3.1	11
50	Structural and photoluminescent properties of nanosized BaMgAl 10 O 17 :Eu 2+ blue-emitting phosphors prepared by sol-gel method. Advances in Natural Sciences: Nanoscience and Nanotechnology, 2015, 6, 035013.	1.5	1
51	Strong luminescence from nanoporous Si with high degree of nanoporous structure by electrochemical etching of Si wafer. Materials Letters, 2015, 142, 126-129.	2.6	3
52	Co-precipitation synthesis and optical properties of green-emitting Ba2MgSi2O7:Eu2+ phosphor. Journal of Luminescence, 2014, 147, 358-362.	3.1	30
53	Monte Carlo Study of Room-Temperature Ferromagnetism in C-Doped ZnO. IEEE Transactions on Magnetics, 2014, 50, 1-4.	2.1	0
54	Near-infrared emission from ZnO nanorods grown by thermal evaporation. Journal of Luminescence, 2014, 156, 199-204.	3.1	44

#	Article	IF	CITATIONS
55	On the origin of green emission in zinc sulfide nanowires prepared by a thermal evaporation method. Journal of Luminescence, 2014, 153, 321-325.	3.1	9
56	Layered structure in core–shell silicon nanowires. Journal of Luminescence, 2014, 154, 46-50.	3.1	5
57	Photoluminescence characteristics of as-synthesized and annealed ZnS:Cu,Al nanocrystals. Advances in Natural Sciences: Nanoscience and Nanotechnology, 2011, 2, 035008.	1.5	19
58	Luminescence Properties of ZnS Nanoparticles and Porous Nanospheres Synthesized via Co-Precipitation and Hydrothermal Route. E-Journal of Surface Science and Nanotechnology, 2011, 9, 521-525.	0.4	3
59	Enhanced Photoelectrochemical Activity of the TiO ₂ /ITO Nanocomposites Grown onto Singleâ€Walled Carbon Nanotubes at a Low Temperature by Nanocluster Deposition. Advanced Materials, 2011, 23, 5557-5562.	21.0	33
60	Novel silver nanoparticles: synthesis, properties and applications. International Journal of Nanotechnology, 2011, 8, 278.	0.2	26
61	Silicon nanowires prepared by thermal evaporation and their photoluminescence properties measured at low temperatures. Advances in Natural Sciences: Nanoscience and Nanotechnology, 2011, 2, 015016.	1.5	10
62	Raman photoluminescence spectra of silicon nanowires synthesized by a vapor phase transport method. Advances in Natural Sciences: Nanoscience and Nanotechnology, 2011, 2, 035004.	1.5	3
63	Photochemical synthesis of highly bactericidal silver nanoparticles. Nanotechnologies in Russia, 2010, 5, 554-563.	0.7	9
64	Green synthesis of finely-dispersed highly bactericidal silver nanoparticles via modified Tollens technique. Current Applied Physics, 2010, 10, 910-916.	2.4	73
65	One-dimensional protuberant optically active ZnO structure fabricated by oxidizing ZnS nanowires. Materials Letters, 2010, 64, 1650-1652.	2.6	16
66	Synthesis of oleic acid-stabilized silver nanoparticles and analysis of their antibacterial activity. Materials Science and Engineering C, 2010, 30, 910-916.	7.3	103
67	Fabrication of a silicon nanostructure-based light emitting device. Journal of Family Business Management, 2010, 1, 025006.	3.4	22
68	Graphene and its one-dimensional patterns: from basic properties towards applications. Advances in Natural Sciences: Nanoscience and Nanotechnology, 2010, 1, 033001.	1.5	6
69	Synthesis of Y ₂ O ₃ :Eu ³⁺ micro- and nanophosphors by sol-gel process. Journal of Physics: Conference Series, 2009, 187, 012074.	0.4	14
70	Er3+/Yb3+-activated silica-hafnia planar waveguides for photonics fabricated by rf-sputtering. Journal of Non-Crystalline Solids, 2009, 355, 1176-1179.	3.1	18
71	Controlled synthesis and luminescence of Eu doped ZnO nanowires and nanorods via hydrothermal method. Journal of Physics: Conference Series, 2009, 187, 012022.	0.4	9
72	Giant magnetoimpedance in layered composite micro-wires for high-sensitivity magnetic sensor applications. Journal of Physics: Conference Series, 2009, 187, 012044.	0.4	6

#	Article	IF	CITATIONS
73	White photoluminescence from Si/SiO ₂ nanostructured film. Physica Status Solidi (B): Basic Research, 2008, 245, 2708-2711.	1.5	О
74	Inclusion of SWCNTs in Nb/Pt co-doped TiO2 thin-film sensor for ethanol vapor detection. Physica E: Low-Dimensional Systems and Nanostructures, 2008, 40, 2950-2958.	2.7	34
75	Mixed SnO2/TiO2 included with carbon nanotubes for gas-sensing application. Physica E: Low-Dimensional Systems and Nanostructures, 2008, 41, 258-263.	2.7	67
76	Erbium-Activated Silica-Hafnia: a Reliable Photonic System. , 2008, , .		2
77	Fabrication and Spectroscopic Properties of Glass-Based Erbium Activated Micro-Nano Photonic Structures. , 2008, , .		1
78	Synthesis and Optical Properties of ZnS Nanostructures. Journal of the Korean Physical Society, 2008, 52, 1562-1565.	0.7	14
79	Nanocomposite Photonic Glasses, Waveguiding Glass Ceramics and Confined Structures Tailoring Er3+ Spectroscopic Properties. , 2007, , .		Ο
80	Structural and optical properties of Si-nanoclusters embedded in silicon dioxide. Physica B: Condensed Matter, 2006, 376-377, 868-871.	2.7	14
81	Magnetic resonance investigation of gold-doped and gold-hydrogen-doped silicon. Physical Review B, 2002, 66, .	3.2	7
82	Complexes of gold and platinum with hydrogen in silicon. Physica B: Condensed Matter, 2001, 302-303, 233-238.	2.7	13
83	Electronic and atomic structure of transition-metal–hydrogen complexes in silicon. Physica B: Condensed Matter, 2001, 308-310, 408-413.	2.7	11
84	Hydrogen passivation of the selenium double donor in silicon:â€,A study by magnetic resonance. Physical Review B, 2000, 61, 7448-7458.	3.2	7
85	Atomic and electronic structure of hydrogen-passivated double selenium donors in silicon. Physica B: Condensed Matter, 1999, 273-274, 239-242.	2.7	2
86	Electron-paramagnetic-resonance studies of defects in electron-irradiated p-type 4H and 6H SiC. Physica B: Condensed Matter, 1999, 273-274, 655-658.	2.7	8
87	High transmittance and excellent hardness TiO ₂ â€SiO ₂ â€Al ₂ O ₃ nanocomposite thin film for antiâ€scratch surface applications. Polymer Composites, 0, , .	4.6	1